Effects of Light Pulse Intensity and Quencher Concentration on the Time-Dependent Fluorescence Quenching Kinetics

Mino Yang, Sangyoub Lee*, Kook Joe Shin, and Kwang Yul Choo†

Department of Chemistry, Seoul National University, Seoul 151-742

Duckhwan Lee

Department of Chemistry, Sogang University, Seoul 121-742. *Received February 18, 1992*

By using the general theoretical framework proposed recently for treating the fluorescence quenching kinetics, we investigate the effect of light pulse intensity on the decay of fluorescence which follows excitation of fluorophors by the light pulse of very short but finite duration. It is seen that conventional theory breaks down when the exciting light pulse has a pulse width comparable to the fluorescent lifetime and its intensity is very high. We also find that even when the light intensity is not too high, conventional theory may fail in either of the following cases: (i) when the quencher concentration is high, (ii) when there is an attractive potential of mean force between the fluorophor and quencher, or (iii) when the energy transfer from the fluorophor to the quencher may also occur at a distance, e.g., *via* dipole-dipole interaction. The validity of the predictions of the present theory may thus be tested by fluorescence quenching experiments performed under such situations.

Introduction

There have been many studies of the quenching of fluorescence from both experimental[1-10] and theoretical perspectives[11-21]. In many experiments[2-8], fluorescent molecules are produced by a light pulse of short duration and the decay of fluorescence intensity from the sample is followed as a function of time. In this paper, we re-examine the various factors which affect the fluorescence decay curve.

We assume that the fluorescence quenching kinetics can be described by the following reaction scheme[11]:

$$D+h\nu_e \xrightarrow{F} D^* \text{ (excitation of fluorophors)} \quad (1.1)$$

$$D^* \xrightarrow{k_F} D+h\nu_F \text{ (fluorophors)} \quad (1.2)$$

$$D^* \xrightarrow{k_{NR}} D \text{ (nonradiative unimolecular decay)} \quad (1.3)$$

$$D^*+A \xrightarrow{k_Q} D+A \text{ (bimolecular quenching)} \quad (1.4)$$

In these equations, F, k_F, k_{NR}, and k_Q represent the rate constants of the respective processes. k_F and k_{NR} may be considered to be independent of time, and their sum, denoted hereafter by k_s, can be determined experimentally as the inverse of the fluorescent lifetime τ_o in the absence of quencher; that is,

$$k_F+k_{NR}\equiv k_S=\tau_o^{-1} \quad (1.5)$$

F in Eq. (1.1), denoting the transition probability per unit time, depends on the intensity of radiation and thus varies with time in general. The bimolecular quenching rate coefficient k_Q in Eq. (1.4) depends on the distribution of the quencher molecules A around D^*. When the relative diffusion between D^* and A is slow, this distribution deviates from the equilibrium one and varies with time, and so does the bimolecular quenching coefficient k_Q.

An important aspect of fluorescence quenching that is neglected in the above reaction scheme is the *static quenching* mechanism[1,2,14] which involves a formation of complex:

$$D+A \rightleftarrows DA \quad (1.6)$$

Although in some cases this mechanism can play an essential part in determining the dependence of fluorescence quenching kinetics on the quencher concentration, we will neglect it for simplicity in the present work.

According to the reaction scheme given by Eqs. (1.1)-(1.4), the time-dependence of the concentration (number density)of D^* molecules will obey the following phenomenological rate law:

$$\frac{d}{dt}[D^*]=-k_s[D^*]+F(t)[D]-k_Q(t)[D^*]C_A^\circ \quad (1.7)$$

where $[D]$ and $[D^*]$ denote the number densities of D and D^* molecules at time, t, respectively, and C_A° is the number density of A molecules that is essentially constant in time. By solving this differential equation, we obtain

$$[D^*]=C_D^\circ\int_0^t d\tau\ F(\tau)\ \exp\Big[-k_S(t-\tau)-\int_\tau^t d\tau_1 F(\tau_1) - C_A^\circ\int_\tau^t d\tau_1 k_Q(\tau_1)\Big] \quad (1.8)$$

where C_D° is the total number density of D molecules. That is, $C_D^\circ=[D^*]+[D]$. The above expression for $[D^*]$ is, however, only formal. We will see below that $k_Q(t)$, being a functional of the nonequilibrium pair distribution of A molecules around D^*, depends on the history of $[D^*]$ variation.

The time-dependence of $[D^*]$ may also be expressed as

$$[D^*]=\int_0^t d\tau F(\tau)[D]G(\tau,\ t) \quad (1.9)$$

Here, $F(\tau)[D]d\tau$ gives the number of D^* molecules generated

*To whom all correspondence should be addressed.
† Deceased January 24, 1991.

in a unit volume between times τ and $\tau+d\tau$, and $G(\tau, t)$ denotes the probability that a D^* molecule excited at time τ remains in the excited state at time t. This is an exact expression. In conventional theories[11], however, it is assumed that each D^* molecule which has been just excited is surrounded by an equilibrium distribution of A molecules and that the A molecule distribution around each D^* follows the same time evolution thereafter. This means that the decay probability of D^* depends only on the time elapsed after excitation regardless of when the excitation occurred. That is, $G(\tau, t)$ in Eq. (1.9) is approximated[11,20] as

$$G(\tau, t)\approx G(t-\tau)= \exp\left[-k_S(t-\tau)-C_A^\circ\int_0^{t-\tau} d\tau_1\, k_Q^{CS}(\tau_1)\right] \quad (1.10)$$

where $k_Q^{CS}(\tau_1)$ is the quenching rate coefficient obtained for the initial condition that each D^* molecule created at $\tau_1=0$ is surrounded by an equilibrium distribution of A molecules. Consequently, it is different from $k_Q(\tau_1)$ in Eq. (18).

In most analyses of experimental data[1-8], one goes one step further by assuming that $[D]\gg[D^*]$ and thus $[D]$ remains nearly constant in time; that is, $[D]\approx C_D^\circ$. Then Eq. (1.9) gives

$$[D^*]=C_D^\circ\int_0^t d\tau F(\tau) \exp\left[-k_S(t-\tau)-C_A^\circ\int_0^{t-\tau} d\tau_1\, k_Q^{CS}(\tau_1)\right] \quad (1.11)$$

Comparison of Eq. (1.11) with Eq. (1.8) shows clearly that the validity of Eq. (1.11) is limited by the condition that $F(\tau)\cong 0$. That is, the intensity of illumination which excites D molecules ought to be weak to ensure that $[D^*]\ll[D]$. One may also question the validity of the approximation made in Eq. (1.10). The assumption that each D^* molecule which has been just excited is surrounded by an equilibrium distribution of A molecules can be true if the D^* molecule has been excited for the first time or re-excited after unimolecular radiative or nonradiative decay as represented by Eq. (1.2) or Eq. (1.3). However, if the re-excited D^* molecule was quenched recently by the bimolecular process [Eq. (1.4)], it will still see, on the average, more A molecules in their vicinity than the equilibrium distribution. For such D^* molecules, the decay law would be different from that given by Eq. (1.10). The opportunity of repeated excitations grows with increases in the intensity and time width of light pulse, and the fraction of D^* molecules re-excited after bimolecular quenching rather than after unimolecular decay increases as the quencher concentration increases. Hence, the conventional theories of fluorescence quenching[11] are expected to break down in such situations.

In the previous works[22,23], we proposed a general theoretical formalism that is free of the above mentioned limitations in conventional theories, and applied it to investigate the effects of quencher on the intensity of fluorescence stimulated by steady-state illumination. In the present work, we study the consequences of the formalism in the analysis of time-resolved fluorescence decay data. In the next section, we first present relevant kinetic equations to describe the quenching dynamics. A numerical procedure to solve the kinetic equations is then described, and the results are compared with the prediction of conventional theories. The final section concludes the present work.

Kinetic Equations

In a previous work[12], starting from a hierarchical system of many-body Smoluchowski equations for the reactant distribution functions[24], we derived the following rate law that is expected for the reaction scheme represented by Eqs. (1.1)-(1.4):

$$\frac{d}{dt}[D^*]=-k_s[D^*]+F(t)[D]-k_Q(t)[D^*][A] \quad (2.1)$$

In the derivation, we were able to show that the time-dependent bimolecular quenching rate coefficient can be evaluated from the following expression:

$$k_Q(t)=\int dr\; 4\pi r^2 S(r)\rho_{AD^*}(r,t). \quad (2.2)$$

Here, $S(r)$ is the sink function which describes the rate of quenching of a D^* molecule when there is an A molecule at the separation of r. $\rho_{AD^*}(r,t)$ is the nonequilibrium pair distribution function; $4\pi r^2 dr\rho_{AD^*}(r,t)[A]$ is the number of A molecules located, on average, in a spherical shell of thickness dr at a distance r from a D^* molecule at time t.

For $t>0$, when the radiation is turned on, the kinetic equation governing the time evolution of $\rho_{AD^*}(r,t)$ is given[22] by

$$\frac{\partial}{\partial t}\rho_{AD^*}(r,t)=L^\circ_{D^*A}\rho_{AD^*}(r,t)-S(r)\rho_{AD^*}(r,t) +F(t)\frac{[D]}{[D^*]}[\rho_{AD}(r,t)-\rho_{AD^*}(r,t)] \quad (2.3)$$

Here, $L^\circ_{D^*A}$ is the Smoluchowski operator for the relative motion of D^* and A and its explicit form is given by

$$L^\circ_{D^*A}=\left(\frac{\partial}{\partial r}+\frac{2}{r}\right)d_{AD^*}(r)\left[\frac{\partial}{\partial r}+\beta\frac{\partial}{\partial r}U_{AD^*}(r)\right] \quad (2.4)$$

where $d_{AD^*}(r)$ is the diffusion coefficient, which depends on r if the hydrodynamic interaction between D^* and A is to be included, and $U_{AD^*}(r)$ is the potential of mean force. $\beta=1/k_BT$ with the Boltzmann constant k_B and the absolute temperature T. If $U_{AD^*}(r)$ has a very steep potential wall at $r=\sigma$, $\rho_{AD^*}(r,t)$ must satisfy the reflecting boundary condition,

$$\left\{d_{AD^*}(r)\left[\frac{\partial}{\partial r}+\beta\frac{\partial}{\partial r}U_{AD^*}(r)\right]\rho_{AD^*}(r,t)\right\}_{r=\sigma}=0 \quad (2.5)$$

On the other hand, as r goes to infinity, $\rho_{AD^*}(r,t)$ approaches unity:

$$\lim_{r\to\infty}\rho_{AD^*}(r,t)=1 \quad (2.6)$$

The initial condition for $\rho_{AD^*}(r,t)$ that corresponds to usual experimental conditions is

$$\rho_{AD^*}(r,t=0)=\exp[-\beta U_{AD^*}(r)] \quad (2.7)$$

The kinetic equation for $\rho_{AD^*}(r,t)$ in Eq. (2.3) involves another nonequilibrium pair distribution function, $\rho_{AD}(r,t)$, which gives the correlation in the distribution of A and ground state D molecules. The kinetic equation governing

the evolution of $\rho_{AD}(r,t)$ for $t>0$ is given[22] by

$$\frac{\partial}{\partial t}\rho_{AD}(r,t)=L_{DA}^{\circ}\rho_{AD}(r,t)+S(r)\frac{[D^*]}{[D]}\rho_{AD^*}(r,t)+\frac{[D^*]}{[D]}[k_S+k_Q(t)C_A^{\circ}][\rho_{AD^*}(r,t)-\rho_{AD}(r,t)] \tag{2.8}$$

where C_A° is the number of A molecules, i.e., $C_A^{\circ}=N_A^{\circ}/V=[A]+[A^*]\cong[A]$ with the number of quencher molecules N_A° and the volume V of the solution. The Smoluchowski operator L_{DA}° for the relative motion of D and A has the same structure as $L_{D^*A}^{\circ}$ in Eq. (2.4), and the boundary and initial conditions for $\rho_{AD}(r,t)$ are also similar to those or $\rho_{AD}(r,t)$ in Eqs. (2.5)-(2.7).

Eqs. (2.1), (2.2), (2.3), and (2.8) constitute the set of integro-differential equations to be solved for the four unknowns, $[D^*]$, $k_Q(t)$, $\rho_{AD^*}(r,t)$, and $\rho_{AD}(r,t)$. We assume that k_S, F, and $S(r)$ are known from quantum mechanical calculations or independent experiments.

However, if the potential of mean force between D^* and A does not differ much from that between D and A [i.e., if $U_{AD^*}(r)\cong U_{AD}(r)$], the problem can be simplified greatly. In such cases, we have

$$[D^*]\rho_{AD^*}(r,t)+[D]\rho_{AD}(r,t)=C_D^{\circ}g^{(2)}(r) \tag{2.9}$$

where C_D° denotes the number density of D molecules including both the excited and the ground state molecules (i.e., $C_D^{\circ}=[D]+[D^*]$), and $g^{(2)}(r)$ is the equilibrium radial distribution function between D and A,

$$g^{(2)}(r)=\exp[-\beta U_{AD}(r)]\cong\exp[-\beta U_{AD^*}(r)] \tag{2.10}$$

With the relation, Eq. (2.9), Eq. (2.3) becomes decoupled from Eq. (2.8) to give

$$\frac{\partial}{\partial t}\rho_{AD^*}(r,t)=L_{D^*A}^{\circ}\rho_{AD^*}(r,t)-S(r)\rho_{AD^*}(r,t)+\{F(t)C_D^{\circ}/[D^*]\}[g^{(2)}(r)-\rho_{AD^*}(r,t)] \tag{2.11}$$

Hence, only this equation together with Eqs. (2.1) and (2.2) has to be solved to obtain reaction kinetic information. Hereafter, we will restrict our discussion to this situation.

Numerical Procedure

We describe a numerical procedure to solve the coupled integro-differential equations, the set of Eqs. (2.1), (2.2), and (2.11). We first transform the real time variable t into a scaled time variable τ into a scaled time variable τ:

$$\tau=t/D \tag{3.1}$$

where D is the relative diffusion coefficient assumed to be a constant with the neglect of hydrodynamic interactions between D^* and A. We then discretize the continuous time domain with sufficiently small time step, $\Delta\tau$, At each time step, we integrate Eq. (2.11) subject to the boundary conditions, Eqs. (2.5) and (2.6), by using the Crank-Nicholson finite difference scheme[25]. The trial value of $[D^*]$ is estimated from the following approximate differnce equation obtained from Eq. (2.1):

$$[D^*]_{j+1}\cong\frac{1-X_j}{1+X_j}[D^*]_j+\frac{D\Delta\tau C_D^{\circ}(F_{j+1}+F_j)}{2(1+X_j)} \tag{3.2}$$

Here, the subscript j denotes the jth time step in time evolution [e.g., F_j denotes the value of $F(t)$ at $t=j\Delta\tau$] and

$$X_j\equiv D\Delta\tau[k_S+(F_{j+1}+F_j)/2+C_A^{\circ}(k_{Q,j+1}+k_{Q,j})/2]/2. \tag{3.3}$$

For the first step, $j=0$, the trial value $[D^*]_1$ is obtained from Eq. (3.2) with the zeroth order estimate for $k_{Q,1}$ given by

$$k_{Q,1}\cong k_{Q,0}=k_Q^{t,0}\equiv\int 4\pi r^2S(r)g^{(2)}(r). \tag{3.4}$$

Then, this value of $[D^*]_1$ is used to calculate $\rho_1(r)$ from Eq. (2.11); $\rho_j(r)$ denotes $\rho_{AD^*}(r,t=j\Delta\tau)$. The resulting $\rho_1(r)$, substituted into Eq. (2.2), gives a refined value for $k_{Q,1}$, which is turn gives a better estimate for $[D^*]_1$ from Eq. (3.2). This iterative procedure is continued until the relative change in the value of $[D^*]_1$ becomes less than a relative error parameter, the value of which is taken to be 1.0×10^{-8} in all calculations reported in this paper.

The same iterative procedure is applied to each time step. That is, the zeroth order estimate for $[D^*]_j$ is obtained from Eq. (3.2) with the approximation, $k_{Q,j}\approx k_{Q,j-1}$. Then, this value of $[D^*]_j$ is used to obtain better estimates for $\rho_j(r)$ and $k_{Q,j}$, ans so on.

Meanwhile, a direct integration of Eq. (2.11) to get the pair distribution function ρ_{AD^*} poses a problem. Since the diffusion space in the radial direction is partitioned into a discrete grid in the finite difference scheme, the outer boundary extended to infinity has to be truncated at a finite separation. To reduce the numerical error due to the truncation, one has to keep as many grid points as possible to ensure sufficient spatial extension of integration range. But this costs large computing time.

To avoid this difficulty, we introduce a nonlinear transformation of the spatial variable given by

$$x=\exp\{-\lambda[(r/\sigma)-1]\} \tag{3.5}$$

where λ is a positive parameter which may be optimized. The optimized value of λ depends on the curvature of pair distribution function in the vicinity of molecular collision surface. λ decreases with the magnitude of the curvature. With this transformation, Eq. (2.11) becomes

$$\frac{\partial\rho}{\partial\tau}=\alpha^2x^2\rho''+\alpha^2x\{x\beta U'-\frac{2}{\lambda-lnx}+1\}\rho'+\left[\alpha^2x\left\{x\beta U'+(1-\frac{2}{\lambda-lnx})U'\right\}-D\{S(x)+\gamma(\tau)\}\right]\rho+D\gamma(\tau)g^{(2)} \tag{3.6}$$

where $\alpha\equiv(\lambda D)/\sigma$, and $\gamma(\tau)\equiv F(\tau)\ C_D^{\circ}/[D^*]$. The prime denotes the differentiation with respect to x.

The sink function $S(x)$ is divided into two parts, a collisional term $S_C(x)$ and a long-ranged interaction terms $S_L(x)$. Imposing the reflecting boundary condition in Eq. (2.5) together with the collisional sink function given by

$$S_C(r)=\kappa_C\delta(r-\sigma)//4\pi\sigma^2 \tag{3.7}$$

is equivalent to imposing a radiative boundary condition given by

$$\left[\rho'+(\beta U'+\frac{\kappa_C}{\lambda k_D})\rho\right]_{x=1}=0 \tag{3.8}$$

where $k_D\equiv4\pi\sigma D$[12]. In these equations, κ_C measures the quen-

ching rate at contact radius. In numerical calculation, it is more convenient to use the radiative boundary condition. Hence we use Eq. (3.6) with $S(x)$ replaced by $S_L(x)$ and the radiative boundary condition given by Eq. (3.8). The outer boundary condition and the initial condition are as given by Eqs. (2.6) and (2.7), respectively.

In the finite difference scheme[25] the transformed diffusion space ($1>x>0$) is partitioned by N grid points, and the continuous pair distribution function $\rho(x,\tau)$ is approximated by a discrete column vector P_i as

$$P_i=\begin{bmatrix} P_{i,1} \\ P_{i,2} \\ P_{i,3} \\ \vdots \\ P_{i,N} \end{bmatrix} \tag{3.9}$$

where the subscript i denotes the ith time step with $t=i\Delta\tau$, and $P_{i,j}$ is the value of the pair distribution function at the jth grid point at the time t. With this discretization, Eq. (3.6) with the associated boundary conditions is equivalent to

$$A \cdot P_{i+1}=B \cdot P_i+G \tag{3.10}$$

Here G is a column vector having N components, and A and B are the $N\times N$ tridiagonal matrices having the following components:

$$A_{i-1,i}=-h(\lambda D/\sigma)^2/2\{x_i^2-\Delta x f(x_i)/2\},$$

$$A_{i,i}=1+h(\lambda D/\sigma)^2/2\{2x_i^2-\Delta x^2 g(x_i,\ \tau_{j+1/2})\},$$

$$A_{i+1,i}=-A_{i-1,i}-h(\lambda D/\sigma)^2 x_i^2,$$

$$B_{i-1,i}=-A_{i-1,i},$$

$$B_{i,i}=2-A_{i,i},$$

$$B_{i+1,i}=-A_{i+1,i},$$

for $2\le i\le N-1$, and

$$A_{1,1}=1+h(\lambda D/\sigma)^2/2\{2x_1^2-\Delta x^2 g(x_1,\ \tau_{j+1/2})\}$$

$$A_{2,1}=-h(\lambda D/\sigma)^2/2\{x_1^2+\Delta x f(x_1)/2\}$$

$$B_{1,1}=2-A_{1,1},$$

$$B_{2,1}=-A_{2,1},$$

$$A_{N-1,N}=-h(\lambda D/\sigma)^2/2\{x_N^2-\Delta x f(x_N)/2\},$$

$$A_{N,N}=1+h(\lambda D/\sigma)^2/2\left\{2x_N^2-\Delta x^2 g(x_N,\ \tau_{j+1/2})-\frac{x_N^2+\Delta x f(x_N)/2}{1+\Delta x\cdot Y}\right\},$$

$$B_{N-1,N}=-A_{N-1,N},$$

$$B_{N,N}=2-A_{N,N}$$

where

$$h\equiv\Delta\tau/\Delta x^2,$$

$$f(x_i)\equiv x\{x\beta U'-\frac{2}{\lambda-lnx}+1\}_{x=x_i},$$

$$g(x_i,\ \tau_{j+1/2})\equiv x[x\beta U''+(1-\frac{2}{\lambda-\ln x})\beta U']-\sigma^2/(\lambda^2 D)[S_L(x)+(\gamma_{j+1}+\gamma_j)/2],$$

$$Y\equiv\beta U'+\kappa_C/\lambda k_D,$$

$$\Delta x=1/(N+1).$$

The elements of vector G are

$$G_1=C(\tau_{j+1/2})g^{(2)}(x_1)+h(\lambda D/\sigma)^2\{x_1^2-\Delta x f(x_1)/2\},$$

$$G_i=C(\tau_{j+1/2})g^{(2)}(x_i)\ (2\le i\le N)$$

where $C(\tau_{j+1/2})\equiv D\Delta\tau[\gamma_{j+1}+\gamma_j]/2$. Here, the prime denotes the derivative with respect to x. The matrix equation, Eq. (3.10), determines the time evolution of the pair distribution function.

To test the accuracy of the present algorithm, we compare long-time results of the numerical calculation with the exact results for the steady state concentration of excited donor molecules under steady illumination. The latter has been obtained analytically in our previous work[22]. The results are presented in Table 1, which shows that the accuracy of the numerical calculation is good enough.

Table 1. Comparison of the Numerical Results for the Steady-state Value of $[D^*]$ Under Steady Illumination with the Exact Result.

$C_A^0(M)$	F	$\mathrm{Log}_{10}[D^*]$	
		Exact	Numerical
0.05	0.1 k_s	−5.384	−5.383
0.05	1.0 k_s	−4.538	−4.537
0.10	0.1 k_s	−5.619	−5.616
0.10	1.0 k_s	−4.722	−4.720
0.30	0.1 k_s	−6.171	−6.166
0.30	1.0 k_s	−5.208	−5.203
0.50	0.1 k_s	−6.494	−6.486
0.50	1.0 k_s	−5.513	−5.505

Model Calculations

We now examine the consequences of the present theory through model calculations. For simplicity the intensity *vs.* time profile of the light pulse is assumed to be given by a function of the form

$$F(t)=(F_o t/t_L)\exp[-(t^4/t_L^4-1)/4] \tag{4.1}$$

The other motional and reaction parameters used in the model calculations are as follows: $T=25$℃, $\tau_o=k_s^{-1}=38.5$ ns, $\sigma=9.1$ Å, $D=5.0\times10^{-7}$ cm^{2}s^{-1} and $k_Q^g=6\times10^{10}$ Lmol^{-1}s$^{-1}=1\times10^{-10}$ cm^{3}s^{-1}.

Effect of Light Pulse Intensity on Fluorescence Decay Curves. Figure 1 displays the effect of ligh pulse intensity on the fluorescence decay curves. For the moment we neglect the interaction potential $U_{AD^*}(r)$ and the long-ranged sink terms $S_L(r)$. The quencher concentration C_A^o has the set equal to 0.1 M. The parameter t_L for the light pulse width appearing in Eq. (4.1) has been set equal to 10 ns.

Both the excitation function $F(t)$ and the fluorescence intensity function $I(t)$, which is proportional to $[D^*]$, increase as the light intensity parameter F_o increases from 0.001 k_s to 10 k_s. However, it is the shape of the fluorescence decay curve rather than the absolute magnitude of the fluorescence

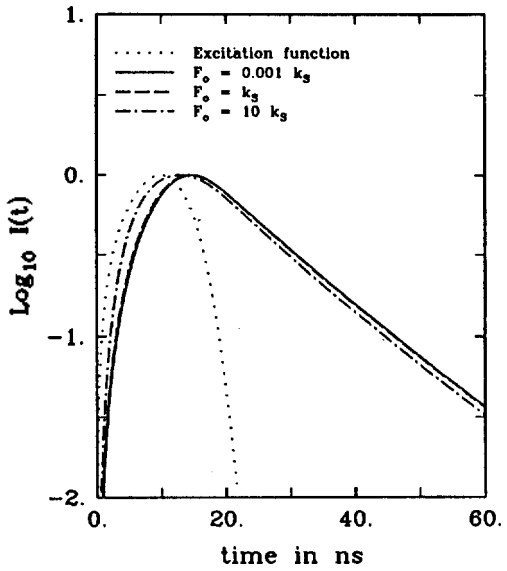

Figure 1. Effect of light pulse intensity on fluorescence decay curves. $I(t)=[D^*][D^*]_{max}$ with $[D^*]_{max}$ denoting the peak concentration of D^*. The dotted curve represents the excitation function $\log_{10}[F(t)/F_o]$. Values of model parameters used are described in the text.

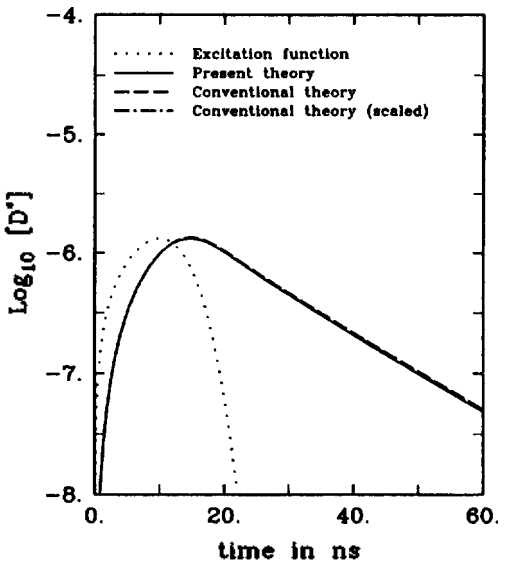

Figure 2. Variation of $[D^*]$ with time when the intensity of light pulse is low. The vartical scale has no meaning for the time profile of excitation function $\log_{10}[F(t)/F_o]$; it has been shifted such that its peak value matches with the peak value of $[D^*]$. Values of model parameters used are described in the text.

intensity that is usually observed in experiments. Hence, in Figure 1 the fluorescence intensity curve for each F_o value has been scaled such that $I(t)=[D^*]/[D^*]_{max}$ with $[D^*]_{max}$ denoting the peak concentration of D^* at the given F_o value. We note that the time at which $I(t)$ becomes maximum shifts to a shorter time as F_o increases.

Comparison with the Conventional Smoluchowski Theory. As mentioned in the introductory section, conventional theories are expected to fail when the duration of light pulse is not so short compared to the life time of fluorophors. The discrepancy between the predictions of the present and conventional theories will be amplified with increases in the light intensity and in the quencher concentration. Indeed, these expectations are observed to be real and the discrepancy between the results of the present and conventional theories is discernible on the quantitative scale.

Results in the Case When $U_{AD^*}(r)=0$ for $r\geq\sigma$ and $S_L(r)=0$. Figure 2 shows that when the quencher concentration is low ($C_A^o=0.1$ M) and excitation rate of D molecules is small with $F_o=0.1\ k_s=2.6\times10^6\ s^{-1}$ and $t_L=10$ ns, the deviation of the conventional theory from the present theory is negligible. However, as the intensity of light increases, the predictions of the conventional theory based on Eq. (1.11) show increasing discrepancy. Figure 3 shows a case when the maximum transition probability of D molecules per unit time, F_o, is ten times as large as k_s (*i.e.*, $F=2.6\times10^8\ s^{-1}$) with other parameters kept at the same values as in Figure 2. The dashed curve representing the result of the conventional theory deviates much from the solid curve representing the result of the present theory. This deviation is largely due to the assumption made by the conventional theory in going from Eq. (1.9) to Eq. (1.11); that is, when the light intensity is high, the concentration of the ground-state D molecules cannot be considered to be constant. In case when

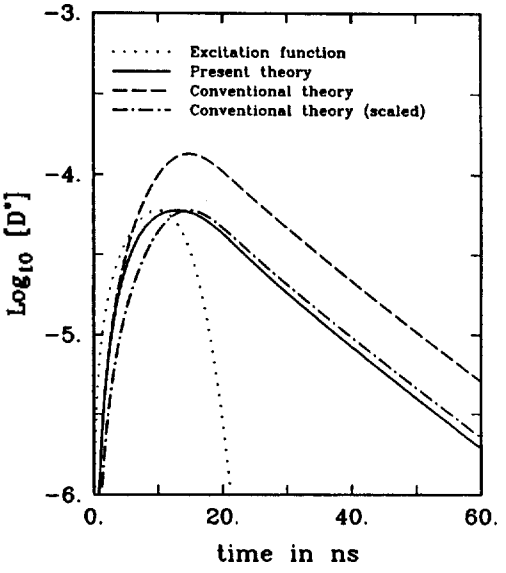

Figure 3. Failure of the conventional theory under high light intensity. Values of model parameters used are described in the text.

the quantity measured in experiments is the variation of the relative intensity of fluorescence rather than the absolute magnitude of $[D^*]$, we also present the results of the conventional theory in such a way that the peak value of $[D^*]$ coincides with the exact one obtained from the present theory. This scaled results with

$$[D^*]_{scaled}=[D^*]_{max}^{present\ theory}\left\{\frac{[D^*]^{conventional\ theory}}{[D^*]_{max}^{conventional\ theory}}\right\} \tag{4.2}$$

are represented by the dot-dashed curve in Figure 3. How-

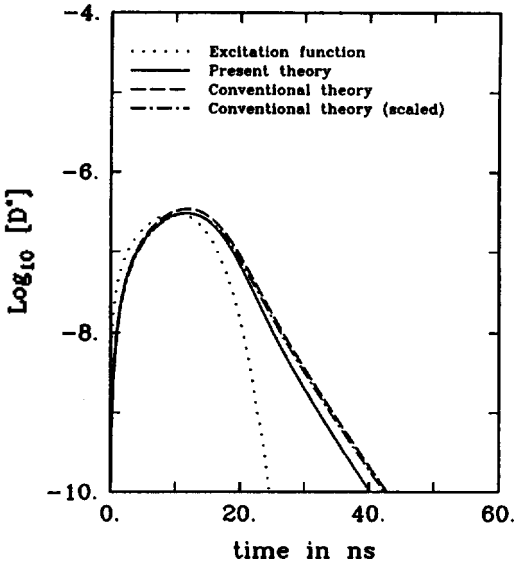

Figure 4. Failure of the conventional theory under high quencher concentration. Values of model parameters used are described in the text.

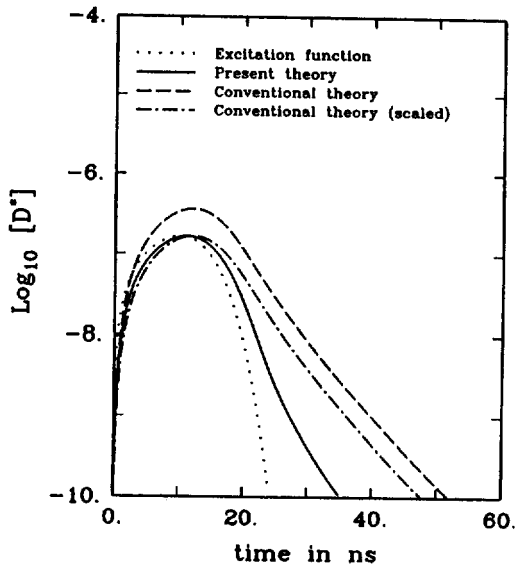

Figure 5. Failure of the conventional theory in the presence of an attractive potential of mean force. Values of model parameters used are described in the text.

ever, we still note a discrepancy. In the conventional and the present theories, the times at which the maximum value of $[D^*]$ or the maximum intensity of fluorescence occurs lag differently from the time at which the exciting light pulse peaks.

Figure 4 shows the deviation of the conventional theory from the present theory under higher quencher concentration ($C_A^\circ=0.5$ M). Increasing the quencher concentration decreases the mean fluorescent life time so that the effect due to the finite time-width of light pulse becomes more discernible. Here, the light intensity is relatively low with $F_o=0.1$ $k_s=2.6\times10^6$ s^{-1} and $t_L=10$ ns; the maximum value of the fraction of D molecules excited is only 0.003. Other parameters were fixed at the same values as in Figure 2. We note that the conventional theory predicts a slower decay of $[D^*]$ or the fluorescence intensity. The failure of the conventional theory in this case is mainly due to the approximation made in Eq. (1.10).

Results in the Case When $U_{AD^*}(r)\neq0$. Figure 5 displays the effect of an attractive Coulomb force on the quenching dynamics. Except that the potential of mean force $U_{AD^*}(r)$ is now given by

$$U_{AD^*}(r)=k_BT(r_c/r) \text{ for } r\geq\sigma \tag{4.3}$$

with $r_c=Z_AZ_De^2/\varepsilon k_BT=-20.0$ Å (Z_Ae and Z_De are charges on A and D molecules, respectively, and ε is the dielectric constant of the solvent), other parameters have the same values as in Figure 2. We see that in this case the conventional theory fails since the approximation made in Eq. (1.10) is inadequate. One may understand this result in terms of the increase in the effective value for the reaction radius. It is well known[11] that effect of the attractive Coulomb interaction in diffusion-influenced reactions can be reproduced by using an effective reaction radius in the potential-free calculation. The value of the effective reaction radius,

$$\sigma_{eff}=r_c[(1+4\pi r_cD/k_Q^{eq})\ \exp(r_c/\sigma)-1]^{-1}, \tag{4.4}$$

is 22.5 Å in the present case. This increase in the effective reaction radius increases the volume fraction, $\phi=4\pi\sigma_{eff}^3C_A^\circ/3$, occupied by the quencher molecules. Since the magnitude of the influence of quencher concentration on the fluorescence quenching kinetics is gauged by this parameter ϕ[11], increase in σ_{eff} results in a similar effect as the increase in C_A°.

Results in the Case When $S_L(r)\neq0$. Effect of long-range energy transfer is shown in Figure 6. We assume that the long-range energy transfer occurs via the dipole-dipole interaction mechanism[11] so that $S_L(r)$ is given by

$$S_L(r)=\tau_o^{-1}(R_o/r)^6 \tag{4.5}$$

where R_o is the critical separation for which energy transfer from D^* to A and unimolecular decay of D^* are equally probable. We set the value of R_o equal to 25 Å. We have assumed that $U_{AD^*}(r)=0$ for $r\geq\sigma$ and other parameters used are the same as in Figure 2. Again, the failure of the conventional Smoluchowski theory may be explained by the increase in the effective reaction radius, which is given[11] by

$$\sigma_{eff}=R_o\frac{(R_o^2/D\tau_o)^{1/4}\Gamma(3/4)}{2\Gamma(5/4)}\left[1+(2^{1/2}/\pi)\cdot\frac{K_{1/4}(z_o)}{I_{1/4}(z_o)}\right]$$

$$\cong0.676(R_o^2/D\tau_o)^{1/4}R_o\left\{1+1.414\ \exp[-R_o^3/(D\tau_o)^{1/2}\sigma^{-2}]\right\}, \tag{4.6}$$

Here, $z_o=(1/2)(R_o^6/D\tau_o)^{1/2}\sigma^{-2}$, $\Gamma(z)$ is the gamma function, and $K_\nu(z)$ and $I_\nu(z)$ are the modified Bessel functions of order ν[26]. For the model calculation in Figure 6, the value of σ_{eff} is 22.7 Å, and this increase in effective reaction radius results in a similar effect as the increase in the quencher concentration.

Concluding Remarks

We have examined the effects of light intensity and quen-

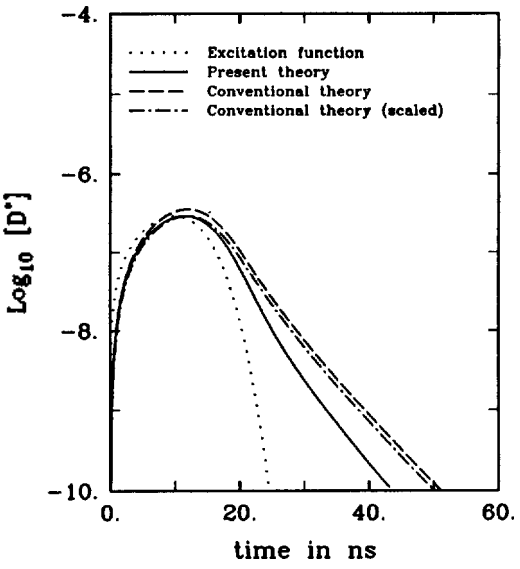

Figure 6. Failure of the conventional theory in the presence of a long-range energy transfer interaction. Values of model parameters used are described in the text

cher concentration on the dacay of fluorescence intensity following an excitation of fluorophors by a light pulse with short but nevertheless finite time width. As expected from physical grounds described in the introductory section, it has been shown that the conventional theory breaks down when the intensity of exciting light pulse is very high and when the quencher concentration is high. We have also found that the presence of an attractive potential of mean force or a long-range energy transfer interaction between the fluorophor and quencher gives rise to a similar effect as the enhancement in the quencher concentration. The validity of the predictions of the present theory may thus be tested by fluorescence quenching experiments performed under such conditions.

Acknowledgement. This work was supported by a grant from the Basic Science Research Program, Ministry of Education of Korea, 1989.

References

1. J. B. Birks, Photophysics of aromatic molecules (Wiley, New York, 1970); J. B. Birks, in: Organic molecular photophysics, ed. J. B. Birks, pp. 409-613 (Wiley, New York, 1975).
2. T. L. Nemzek and W. R. Ware, *J. Chem. Phys.* **62**, 477 (1975).
3. D. P. Millar, R. J. Robbins, and A. H. Zewail, *J. Chem. Phys.* **75**, 3649 (1981).
4. R. W. Wijnaendts van Resandt, *Chem. Phys. Letters*, **95**, 205 (1983).
5. N. Tamai, T. Yamazaki, I. Yamazaki, and N. Mataga, *Chem. Phys. Letters*, **120**, 24 (1985).
6. J. R. Lakowicz, M. L. Johnson, I. Gryczynski, N. Joshi, and G. Laczko, *J. Phys. Chem.*, **91**, 3277 (1987).
7. N. Periasamy, S. Doraiswamy, B. Venkataraman, and G. R. Fleming, *J. Chem. Phys.* **89**, 4799 (1988).
8. G. C. Joshi, R. Bhatnagar, S. Doraiswamy, and N. Periasamy, *J. Phys. Chem.* **94**, 2908 (1990).
9. F. Heisel and J. A. Miehe, *J. Chem. Phys.* **77**, 2558 (1982).
10. J. K. Baird and S. P. Escott, *J. Chem. Phys.* **74**, 6993 (1981).
11. S. A. Rice, Diffusion-limited reactions in comprehensive chemical kinetics, Vol. 25, eds. C. H. Bamford, C. F. H. Tipper, and R. G. Compton (Elsevier, Amsterdam, 19 85).
12. G. Wilemski and M. Fixman, *J. Chem. Phys.* **58**, 4009 (1973).
13. U. Gösele, M. Hauser, U. K. A. Klein, and R. Frey, *Chem. Phys. Letters*, **34**, 519 (1975).
14. J. K. Barid, J. S. McCaskill, and N. Y. March, *J. Chem. Phys.* **74**, 6812 (1981); *ibid.*, **78**, 6598 (1983).
15. J. Keizer, *J. Phys. Chem.*, **86**, 5052 (1982); J. Keizer, *Chem. Rev.*, **87**, 167 (1987).
16. J. Keizer, *J. Am. Chem. Soc.*, **105**, 1494 (1983), **107**, 5319 (1985).
17. R. I. Cukier, *J. Chem. Phys.* **82**, 5457 (1985).
18. B. Stevens, *Chem. Phys. Letters*, **134**, 519 (1987).
19. J. Najbar, *Chem. Phys.* **120**, 367 (1988).
20. A. Szabo, *J. Phys. Chem.*, **93**, 6929 (1989).
21. H. Zhou and A. Szabo, *J. Chem. Phys.* **92**, 3874 (1990).
22. S. Lee, M. Yang, K. J. Shin, K. Y. Choo, and D. Lee, *Chem. Phys.* **156**, 339 (1991).
23. M. Yang, S. Lee, K. J. Shin, K. Y. Choo, and D. Lee, *Bull. Korean Chem. Soc.* **12**, 414 (1991).
24. S. Lee and M. Karplus, *J. Chem. Phys.*, **86**, 1883 (1987).
25. W. H. Press, B. P. Flannery, S. A. Teukolsky, and W. T. Vetterling, Numerical recipes (Cambridge Univ., Cambridge, 1986).
26. M. Abramowitz and I. A. Stegun, Handbook of mathematical functions (Dover, New York, 1970).